

***In Vivo* Brain Tumor Demarcation Using Optical Spectroscopy[¶]**

Wei-Chiang Lin^{*1}, Steven A. Toms², Mahlon Johnson³, E. Duco Jansen^{1,2} and Anita Mahadevan-Jansen^{1,2}

Departments of ¹Biomedical Engineering, ²Neurological Surgery and ³Pathology, Vanderbilt University, Nashville, TN

Received 5 September; accepted January 2001

ABSTRACT

The applicability of optical spectroscopy for intraoperative detection of brain tumors/tumor margins was investigated in a pilot clinical trial consisting of 26 brain tumor patients. The results of this clinical trial suggest that brain tumors and infiltrating tumor margins (ITM) can be effectively separated from normal brain tissues *in vivo* using combined autofluorescence and diffuse-reflectance spectroscopy. A two-step empirical discrimination algorithm based on autofluorescence and diffuse reflectance at 460 and 625 nm was developed. This algorithm yields a sensitivity and specificity of 100 and 76%, respectively, in differentiating ITM from normal brain tissues. Blood contamination was found to be a major obstacle that attenuates the accuracy of brain tumor demarcation using optical spectroscopy. Overall, this study indicates that optical spectroscopy has the potential to guide brain tumor resection intraoperatively with high sensitivity.

INTRODUCTION

Surgical removal of brain tumors is the most common initial treatment received by brain tumor patients (1,2). Surgical resection can benefit the patients in several ways: for example, it relieves the mass effect of tumor on neurological tissue and allows histological diagnosis of the tumor, which directly affects the direction of follow-up therapeutic strategy (3). Many studies have demonstrated that aggressive surgical resection enhances the survival length and quality of life for brain tumor patients (4,5). Therefore, the goal of brain tumor resection procedures is to maximize tumor removal with minimal neurological damage. To achieve this goal accurate intraoperative identification of brain tumor margins during craniotomy is required.

Intraoperatively, brain tumor margins are currently determined by neurosurgeons by visual inspection and information provided by surgical navigation systems that are based

on computerized tomography (CT)†/magnetic resonance (MR) images (6) and/or intraoperative ultrasound (IOUS) (7). However, these techniques have several limitations that prevent surgeons from achieving a complete tumor resection. First, the true infiltrating margins of primary tumors may not be visible on CT/MR images, even T2-weighted MR images, unless the tumor cells are sufficiently dense. Secondly, registration errors and intraoperative brain shift can degrade the spatial accuracy of the surgical navigation system by as much as 1 cm (8,9). Thirdly, gliomas, unlike most metastatic tumors, do not typically possess clear boundaries, *i.e.* the margins appear blurred in the IOUS images. Fourthly, it is often difficult, even for experienced neurosurgeons, to visually differentiate low-grade gliomas and associated tumor margins from normal brain tissues. Although on-site pathology provides accurate diagnosis, it is time-consuming and expensive and as such is not used routinely for tumor-margin detection. Hence, there is a clear need for the development of a real-time, guidance tool that allows intraoperative detection of brain tumor margins with high sensitivity to facilitate complete or high-degree brain tumor resection. Optical spectroscopy has the potential to fulfill this need.

Tissue diagnosis using optical spectroscopy, also known as optical biopsy, has been widely investigated by several research groups in various organ systems *in vivo* (10,11). However, very few studies have been reported on the feasibility of optical spectroscopy for brain tumor differentiation/demarcation. Bottiroli *et al.* (12) reported that *in vivo* brain tissue differentiation may be achieved using the peak location and line shape of fluorescence emission at 340 nm excitation. As the number of patients presented in this study was limited, the applicability of fluorescence spectroscopy for *in vivo* brain tumor demarcation was not truly validated. The feasibility of using 5-aminolevulinic acid (ALA)-induced fluorescence to assist in brain tumor resection was studied by Stummer *et al.* (13) in a human clinical trial. Results from this study show that ALA fluorescence can predict the presence of tumor tissue with a sensitivity of 85% and a specificity of 100% with respect to histology. How-

[¶]Posted on the website on 16 February 2001.

^{*}To whom correspondence should be addressed at: Stevenson Center 5801, Department of Biomedical Engineering, Vanderbilt University, P.O. Box 351631, Station B, Nashville, TN 37235, USA. Fax: 615-343-7919; e-mail: linw@vuse.vanderbilt.edu

© 2001 American Society for Photobiology 0031-8655/01 \$5.00+0.00

[†]**Abbreviations:** ALA, 5-aminolevulinic acid; CCD, charge-coupled device; CT, computerized tomography; c.u., calibrated units; FWHM, full width at half maximum; GBM, glioblastoma multiforme; IOUS, intraoperative ultrasound; ITM, infiltrating tumor margin; MR, magnetic resonance; NIST, National Institute of Standards and Technology; VUMC, Vanderbilt University Medical Center.

ever, low-grade tumors and tumor margins could not be identified in this study, as ALA was not taken up by tumor cells in areas with an intact blood-brain barrier. Moreover, the effectiveness of ALA-induced fluorescence is limited by photobleaching. Thus, these problems diminish the capability of ALA-induced fluorescence for brain tumor demarcation.

In an initial *in vitro* study we examined the feasibility of using combined optical spectroscopy (*i.e.* fluorescence and diffuse reflectance spectroscopy) to differentiate brain tumors from normal brain tissues. A sensitivity and specificity of 95 and 90%, respectively, were achieved (14). Despite its success the ability of optical spectroscopy for brain tumor margin detection was not fully investigated, as it was not feasible to obtain suitable brain samples with infiltrating tumor cells. In addition, the spectral properties of different brain-tissue types need to be characterized *in vivo*. A pilot clinical study was thus designed to address these issues.

In this paper, the clinical applicability of combined autofluorescence and diffuse-reflectance spectroscopy for brain tumor demarcation was investigated, and the results of this study are presented here. *In vivo* fluorescence and diffuse-reflectance spectra were acquired from areas of normal brain tissues, brain tumors and tumor margins in 26 patients undergoing brain tumor resection. Tissue spectra of different brain-tissue types were characterized and compared to those reported *in vitro*. Discrimination algorithms based on the observed spectral features were developed to differentiate normal brain tissues from brain tumors. Moreover, the capability of optical spectroscopy in detecting the infiltrating tumor margins (ITM) was examined.

MATERIALS AND METHODS

The pilot clinical study described in this paper was conducted at the Vanderbilt University Medical Center (VUMC) with prior approval from the Vanderbilt University Institutional Review Board. All adult brain tumor patients receiving craniotomies at VUMC were considered and recruited irrespective of gender or race. The final eligibility of each patient was determined by the participating neurosurgeon (S.A.T.) based on the tumor type, tumor location and medical condition of the patient such that patient care was not compromised. Written consent was obtained from each enrolled brain tumor patient prior to the surgery.

In vivo optical spectra of brain tissues were acquired using a portable spectroscopic system. A high-pressure nitrogen laser at 337 nm (Nitrogen Laser 79070; Oriol Corporation, Stratford, CT) was used as the excitation source for fluorescence spectroscopy, a 150 W halogen lamp (Fiber Lite 180; Edmund Scientific, Barrington, NJ) for diffuse-reflectance spectroscopy. Light delivery and collection were achieved *via* a fiberoptic probe (custom-designed by Visionex, Inc., Atlanta, GA). This probe consists of seven 300 μm core-diameter optical fibers: a central conventional fiber is surrounded by six beam-steered fibers which enhance the collection efficiency of the probe (15). Two of the surrounding fibers at 6 and 12 o'clock in the probe were used to deliver the laser and white light, respectively, to the tissue; the remaining fibers were used to collect the fluorescence as well as the reflected light.

The light collected by the probe was dispersed by a spectrograph (Triax 180; Instruments S.A., Inc., Edison, NJ) with a 300 gr/mm grating and detected by a thermoelectrically cooled charge-coupled device (CCD) camera (2000 \times 800 pixels, Spectrum One; Instruments S.A.). A 100 μm slit was used at the entrance of the spectrograph yielding a spectral resolution of 1.6 nm. Both the spectrograph and the CCD camera were controlled by a laptop computer *via* an IEEE-488 controller. Two 360 nm longpass filters (360LP; Omega Optical, Brattleboro, VT) were placed in front of the entrance slit

of the spectrograph to reject the reflected laser light collected by the probe. A medical-grade isolation transformer (IT1500-4; Dale Technology Corporation, New York) was used with the portable spectroscopic system to comply with the electrical safety standard of the operating room.

A standard protocol was designed for the spectral measurements and maintained for all the patients in this study. Measurements were performed intraoperatively by the participating neurosurgeon. The fiberoptic probe was sterilized using either gas or a low-temperature plasma-based method, causing no structural or functional damage to the optical probe, prior to each patient study. Multiple sites with tumors, tumor margins and normal brain tissues were studied during the tumor-resection procedure. The total number of investigated sites in each patient varied from five to ten, depending on the complexity of tumor resection involved and the medical condition of the patient. Prior to spectral acquisition each investigated site was rinsed with saline to remove any blood accumulated at the tissue surface. The optical probe was then placed lightly in direct contact with the target tissue and three spectra: background $B(\lambda)$ (*i.e.* measured without light source), fluorescence $F(\lambda)$ and diffuse-reflectance $R_d(\lambda)$ were sequentially acquired. The output power of the white-light source was maintained at 0.6 mW, and the nitrogen laser was operated at 20 Hz repetition rate, 5 ns pulse width and average pulse energy of $45 \pm 5 \mu\text{J}$. An integration time of 1 s was used for each spectral measurement. Spectral acquisition at a given site took approximately 30 s to complete; this is mainly attributed to instrumentation delays introduced in the spectroscopic system (*e.g.* refreshing the readout buffer of the CCD camera) between consecutive spectral measurements. The overhead room lights in the operating room were temporarily turned off during spectral acquisition, while the surgical lights were left on but pointed away from the operating field. This minimizes the contribution of the ambient light in the acquired optical spectra while maintaining a comfortable light level for the surgeons and staff in the operating room. Following spectral acquisition the investigated site was typically registered on the preoperative CT or MR images by the surgical navigation system (Viewpoint; Picker International, Highland Heights, OH) to record its location. A biopsy was then taken from the investigated site except when the site was identified to be grossly normal or was in the functional area of the brain. Biopsy samples from the initial 14 patients were stored in an ultra-low-temperature freezer until histopathological examination. However, histological identities of more than 30% of these samples could not be determined by the neuropathologist due to excessive freezing artifacts. Subsequently, biopsy samples were fixed in formalin upon excision.

At the end of each patient study the reference spectra, $F_{\text{ref}}(\lambda)$ and $R_{d,\text{ref}}(\lambda)$ were measured from a fluorescence and a reflectance standard to monitor interpatient variability in laser-pulse energy, white-light power and other instrumental parameters. The fluorescence standard is a low-concentration Rhodamine 6G solution (2 mg/L) contained in a quartz cuvette. The reflectance standard is a 20% reflectance plate (Labsphere, North Sutton, NH) placed in a black box.

Before the spectral analyses all raw spectra were processed to eliminate any instrument-introduced variations. Background subtraction was first performed on all fluorescence and diffuse-reflectance spectra with the corresponding background spectra. A compensation factor, $C_{f,i}$ (or $C_{R_d,i}$), which accounts for the interpatient variations in the instrument parameters was then multiplied to each background-subtracted spectrum. $C_{f,i}$ (or $C_{R_d,i}$) is determined by taking the ratio of the reference spectrum recorded for the *i*-th patient to that of the first patient for a given wavelength. That is,

$$C_{f,i} = F_{\text{ref},i}(\lambda_f)/F_{\text{ref},1}(\lambda_f) \quad \text{and}$$

$$C_{R_d,i} = R_{d,\text{ref},i}(\lambda_{R_d})/R_{d,\text{ref},1}(\lambda_{R_d}),$$

where $\lambda_f = 560 \text{ nm}$ and $\lambda_{R_d} = 700 \text{ nm}$.

All fluorescence spectra were further corrected for the nonuniform spectral response of the detection system using calibration factors $D_f(\lambda)$ generated using a National Institute of Standards and Technology (NIST) traceable calibrated tungsten-ribbon filament lamp. Reflectance spectra, on the other hand, were calibrated using the factors $D_{R_d}(\lambda)$ derived from the reflectance measurement of a mirror (10R08ER.1; Newport Corporation, Irvine, CA) with a known wave-

Table 1. Histopathological distribution of 120 investigated samples in the pilot clinical study

Category	# of sites	# of patients
Normal	21	8*
Infiltrating tumor margins	27	19
Primary tumors	60	
Secondary tumors	12	7

*From both primary and secondary tumor patients.

length-dependent reflectivity. It should be noted that $D_{Rd}(\lambda)$ account for not only the nonuniform spectral response of the detection system but also the nonuniform spectral emission of the halogen light source.

Spectral data from investigated sites which did not have a confirmed histopathologic diagnosis were excluded from further analyses. Furthermore, spectral sets showing excessive blood absorption, determined by the criterion $\rightarrow Rd(550\text{ nm}) < 150$ calibrated units [c.u.], were also rejected. The remaining spectral data set was then divided into four major categories: normal brain tissues, primary tumors, secondary tumors and ITM, based on their histopathologic identities. Analyses were performed to characterize the spectral difference between the various brain-tissue categories. A Student's *t*-test was performed on the spectral intensity, peak position and line shape to see if any observed differences in these spectral parameters between tissue categories were statistically significant. Statistically significant differences in the *in vivo* fluorescence and reflectance spectra between the different tissue categories were then used to develop discrimination algorithms. It should be noted that the focus of this analysis was to optimize the separation of tumor margins from normal brain tissues. In addition, *in vivo* tissue optical spectra were compared to those acquired *in vitro*.

RESULTS

Twenty-six brain tumor patients were enrolled in this pilot clinical study over a period of 10 months. All the patients in this study, though recruited irrespective of race, were Caucasians. The patient population consisted of 15 males and 11 females; the majority of these patients were between the ages of 30 and 50. Of the 26 patients studied 19 had primary tumors and seven, secondary tumors. A total of 120 measurement sites were retained for the spectral analyses; the histopathological distribution of these sites as determined by the neuropathologist are shown in Table 1.

Figure 1 illustrates the *in vivo* spectra obtained from a typical patient. In general, the lineshape of the *in vivo* fluorescence and diffuse-reflectance spectra of brain tissues strongly resembles that of the spectra acquired *in vitro* (14). Peak fluorescence in the majority of *in vivo* brain tissues occurred between 455 and 480 nm. The fluorescence intensities at 460 nm (F_{460}) of all the samples were compared between different tissue categories, and the results are shown in Table 2. The difference in F_{460} between normal brain tissues and brain tumors was found to be statistically significant only when comparing gray matter with tumor margins, anaplastic gliomas and oligodendrogliomas. Although some differences were observed, F_{460} alone could not accurately differentiate between the various brain-tissue types *in vivo*.

The variations in the lineshape of *in vivo* fluorescence spectra, with respect to the primary peak position and full width half maximum (FWHM), were also compared among the different brain tissue categories. The results from these analyses are shown in Table 2. Statistically significant var-

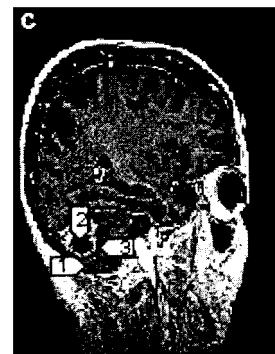
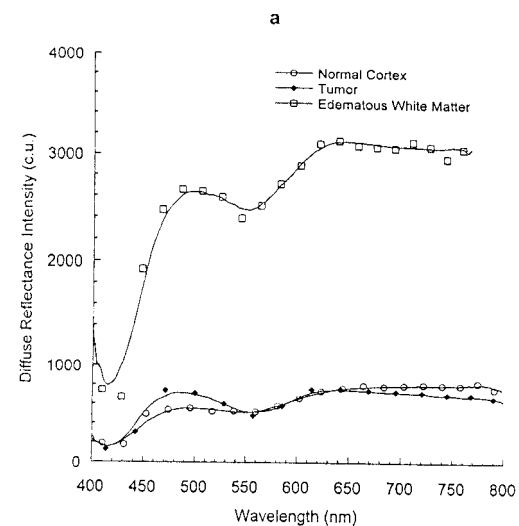
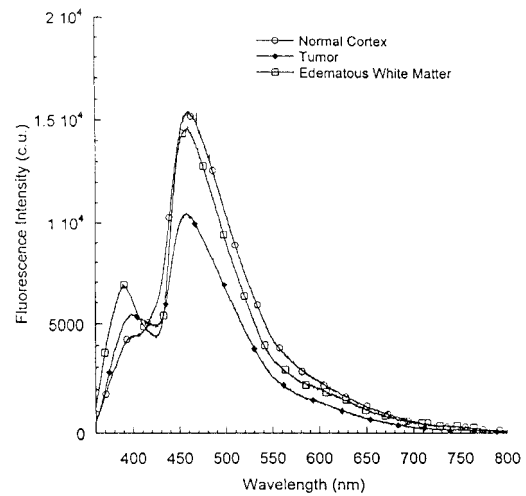


Figure 1. Typical optical spectra obtained from a tumor patient (secondary tumor): (a) fluorescence spectra, (b) diffuse-reflectance spectra, and (c) spatial registrations of investigated sites on MR image. Only three of seven investigated sites from this patient are shown. The units c.u. refer to calibrated units (calibrated with respect to an NIST calibrated tungsten lamp).

iations in the primary peak location were only found between normal white matter and two of the primary tumors (anaplastic glioma and oligodendroglioma). In addition, the comparison showed no evidence of a red-shift in the fluo-

Table 2. *In vivo* fluorescence spectral comparison

Tumor	Normal	F ₄₆₀	Peak	FWHM
		intensity <i>p</i> -value	position <i>p</i> -value	
Infiltrating tumor margins	White	0.9654	0.4055	0.0136
	Gray	0.0745	0.5135	0.8277
Primary tumors				
Astrocytoma	White	0.1469	0.9256	0.0369
	Gray	0.9648	0.1051	0.0003
Anaplastic glioma	White	0.2634	0.0230	0.0101
	Gray	0.0167	0.4686	0.8057
Glioblastoma multi- forme	White	0.8288	0.9873	0.0639
	Gray	0.1261	0.1069	0.3680
Oligodendroglioma	White	0.4714	0.0305	0.2068
	Gray	0.0536	0.8496	0.0171
Secondary tumors				
	White	0.1455	0.5266	0.0016
	Gray	0.8304	0.1153	0.1786

rescence spectra of glioblastoma multiforme (GBM) sites as compared with normal tissues, as reported previously by Bottiroli *et al.* (12). Hence, the position of the primary fluorescence peak alone could not be used to differentiate consistently between the different brain-tissue categories. The average FWHM of the primary fluorescence peak of normal white matter was found to be less than that of all tumors except oligodendrogliomas. In addition, the average FWHM of normal gray matter was statistically different only when compared with that of anaplastic astrocytomas and oligodendrogliomas.

Diffuse reflectance (Rd) of brain tissues decreased gradually from 650 to 800 nm, similar to that observed *in vitro*, when the signatures of blood absorption in Rd were not pronounced. Signatures of either oxyhemoglobin or deoxyhemoglobin absorption (*i.e.* blood absorption) were frequently observed in the *in vivo* diffuse-reflectance spectra (see Fig. 1b). In addition, the degree of blood absorption, as evidenced by the slope of Rd(λ) between 580 and 600 nm, was found to be more pronounced *in vivo* than *in vitro*. Normal white matter and tumor margins involving white matter demonstrate strong diffuse reflectance between 600 and 800 nm. Some primary tumors involving oligodendrocytes also show strong reflectance between 600 and 800 nm.

Various empirical discrimination algorithms, utilizing the statistically significant spectral variations observed, were developed and tested to determine their performance in separating normal brain tissues from each of the remaining tissue categories. Successful empirical algorithms previously developed *in vitro* (14) were first applied to test their validity *in vivo*. It was observed that the *in vitro* discrimination algorithm based on fluorescence intensity alone (*i.e.* F₄₆₀) could not be used to differentiate between normal and tumor brain tissues *in vivo* (Table 2). However, the *in vitro* discrimination algorithm based on the ratio of the fluorescence and diffuse reflectance intensity at 460 nm (F/Rd₄₆₀) and the diffuse reflectance intensity at 625 nm (Rd₆₂₅) could be used to differentiate normal brain tissues from brain tumors, especially ITM, *in vivo* with good accuracy. A sensitivity of 81% and a specificity of 76% were achieved in separating normal brain tissues from ITM (see Fig. 2a). Five ITM sam-

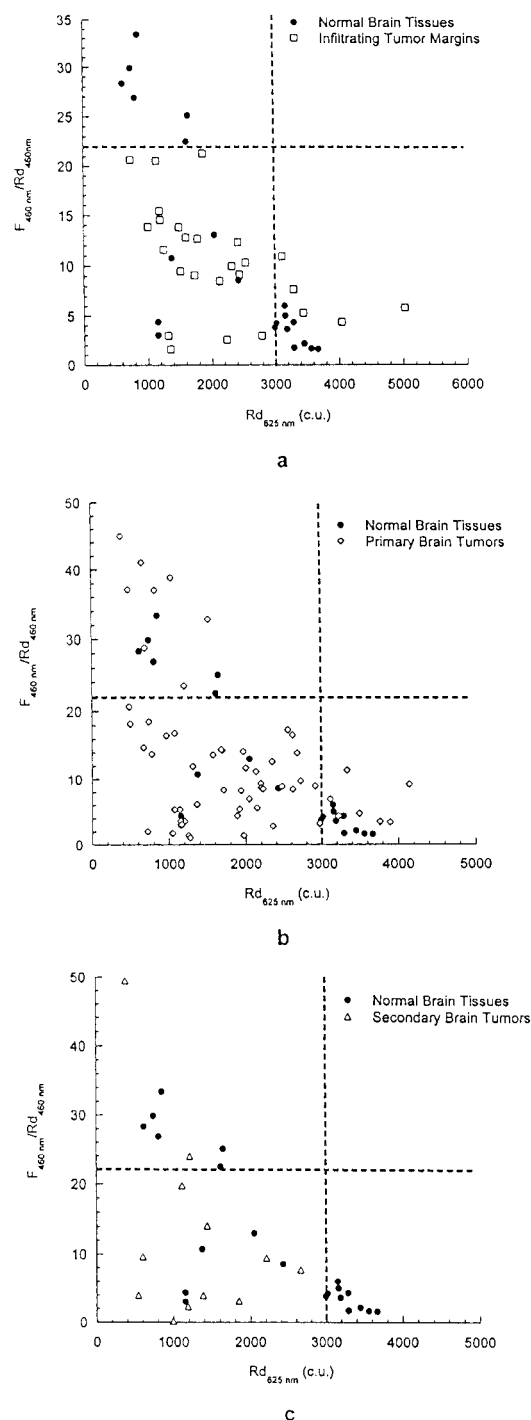


Figure 2. Scatter plots of F/Rd₄₆₀ vs Rd₆₂₅ in the single-step algorithm for normal brain tissues and: (a) ITM, (b) primary tumors, and (c) secondary tumors. The dash lines (F/Rd₄₆₀ = 22 and Rd₆₂₅ = 3000 c.u.) represent the discrimination lines used.

ples were misclassified along the Rd₆₂₅ axis, three of which were from patients with tumors involving oligodendrocytes and two from patients with GBM. All five misclassified normal brain samples were cortical tissues. The same discrimination algorithm could also be used to separate normal tissues from primary tumors with a sensitivity of 75% (see Fig. 2b). Of the 15 misclassified primary tumor samples, there

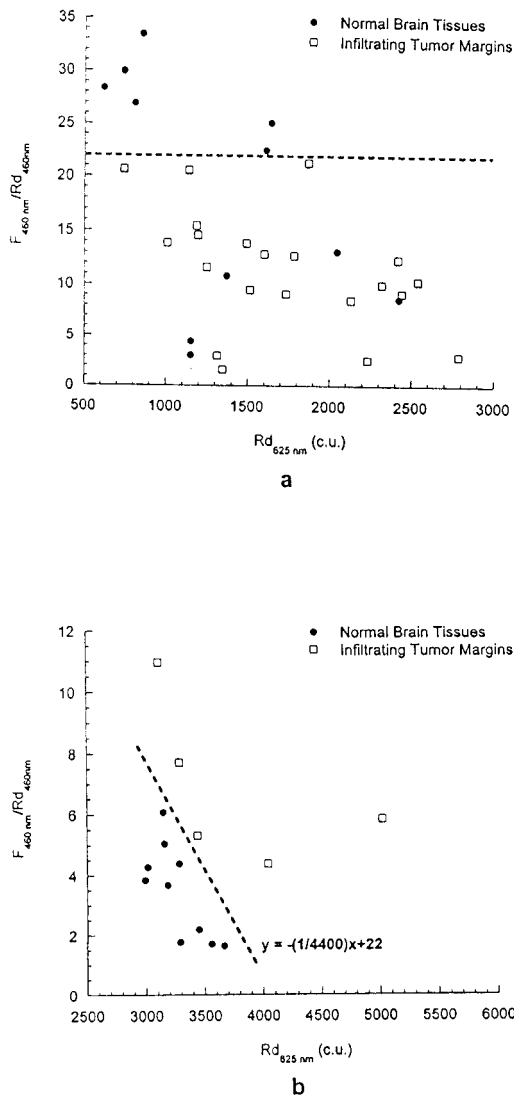


Figure 3. Scatter plots of F/Rd_{460} vs Rd_{625} representing step 2 in the two-step algorithm for: (a) samples with low reflectance ($Rd_{625} \leq 3000$ c.u.), and (b) samples with high reflectance ($Rd_{625} > 3000$ c.u.) within normal brain tissues and ITM.

were eight oligodendrogliomas, five glioblastomas, one anaplastic astrocytoma and one embryonal neoplasm. Moreover, four of the 15 misclassified tumor samples were from a single patient. A sensitivity of 83% was obtained in separating secondary tumors from normal brain tissues using the same method, as shown in Fig. 2c. Two tumor samples misclassified along the F/Rd_{460} axis were from a patient with metastatic colon cancer. Thus, using this algorithm an overall sensitivity of 78% and specificity of 76% were achieved.

Based on the results of the spectral-data analyses described earlier and the single-step discrimination algorithm a two-step discrimination algorithm was developed using F/Rd_{460} and Rd_{625} . In this method the entire *in vivo* spectra were first divided into two subgroups based on Rd_{625} . Those samples with low Rd_{625} (*i.e.* $Rd_{625} \leq 3000$ c.u.) were then discriminated using an F/Rd_{460} of 22 as the cutoff (Figs. 3a and 4a); samples above the cutoff were classified as normal and those under as tumorous. The samples with high Rd_{625}

(*i.e.* $Rd_{625} > 3000$ c.u.) were then screened using a linear cutoff that intersects the F/Rd_{460} axis at 22 and Rd_{625} at 4400 c.u. (Figs. 3b and 4b); samples located above the discrimination line were classified as tumorous and those located below as normal. Overall, this two-step discrimination method performed better than the single-step discrimination method, which was mainly attributed to the reduction in misclassifications along the Rd_{625} axis. The most significant improvement using this new algorithm was found in separating normal brain samples from ITM, where a sensitivity of 100% was achieved. Sensitivity improved from 75 to 84% in separating normal brain tissues from primary tumors using the new algorithm. However, no improvement was obtained in separating normal brain tissues from secondary tumors using the two-step algorithm. An overall sensitivity of 89% and specificity of 76% was achieved using the two-step algorithm.

DISCUSSION

The pilot clinical study described here demonstrates the potential of optical spectroscopy for brain tumor demarcation *in vivo*. The results of this study validate the results of our previous *in vitro* study (14), where normal brain tissues could be separated from tumor tissues accurately using combined fluorescence and diffuse-reflectance spectroscopy. Normal and tumor-bearing brain tissues can be differentiated *in vivo* using optical spectroscopy with an average sensitivity of 89% and specificity of 76% using a two-step empirical discrimination algorithm. More importantly, this study proves the effectiveness of optical spectroscopy in differentiating normal brain tissues from ITM with 100% sensitivity. Although not specifically addressed in this paper, optical spectroscopy was also found to be more sensitive in detecting ITM as compared with existing techniques used in current practice. On several occasions, investigated brain tissues, identified as tumor or margin based on their optical spectra but not in CT/MR and ultrasound images and/or on visual inspection, were later histologically determined to be either solid tumors or ITM. Overall, the results of this study strongly support the hypothesis that optical spectroscopy is capable of providing accurate brain tumor demarcation and can be used as an effective intraoperative tool for the guidance of tumor resection.

In vivo fluorescence spectra from those brain tissues with little or no influence from blood absorption showed only one emission peak (between 455 and 480 nm) over the entire measured spectral region (*i.e.* 360–800 nm). However, many investigated sites had medium to high blood content, as indicated by the blood-absorption signatures in their diffuse-reflectance spectra; hence, their fluorescence spectra have two emission peaks (see Fig. 1a). The red-shift in the position of the primary fluorescence maxima in GBM tissues as compared to normal tissues (12) was not observed in this study. In addition, the broadening of fluorescence spectra observed in GBM as compared to normal brain tissues (12) was not confirmed in this *in vivo* study. According to the analysis performed on the FWHM of the primary fluorescence peak, the spectra of several tumor types, including tumor margins, were found to be broader as compared with those of white matter (indicated in Table 2). However, the

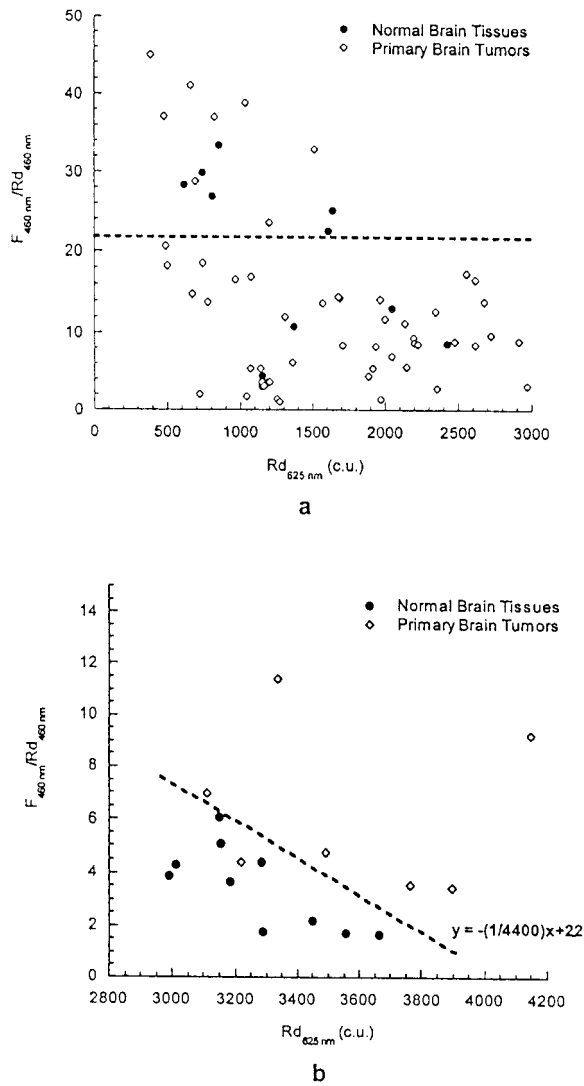


Figure 4. Scatter plots of F/Rd_{460} vs Rd_{625} representing step 2 in the two-step algorithm for: (a) samples with low reflectance ($Rd_{625} \leq 3000$ c.u.), and (b) samples with high reflectance ($Rd_{625} > 3000$ c.u.) within normal brain tissues and primary tumors.

variations in the primary peak position or FWHM were not consistent for the four brain-tissue categories defined in this study and hence could not be used as reliable discrimination criteria.

F_{460} alone was insufficient as a discrimination criterion *in vivo* despite its success *in vitro*. This variability is mainly attributed to the inherently bloody nature (*i.e.* strong blood absorption) of the operating field under which the current study was conducted. It is well known that the intensity of tissue fluorescence is modulated by the presence of blood absorption. More specifically, a superficial layer of blood present at the surface of the investigated site may cause significant attenuation of both the excitation and the emission light, leading to a drastic attenuation of the tissue fluorescence. This phenomenon manifests itself as valleys at 420, 540 and 580 nm in the diffuse-reflectance spectra as well as in the fluorescence spectra. Thus, strong blood contamination modulates the shape of the tissue fluorescence spectra (see Fig. 1a), which may explain why consistent variations

in terms of the peak position and FWHM of fluorescence spectra could not be observed between normal brain tissues and brain tumors.

The scattering coefficient of white matter is typically much greater than those of gray matter and brain tumors (16; W.-C. Lin, unpublished). Hence, the diffuse reflectance (*i.e.* Rd_{625}) of white matter is expected to be higher than that of tumor tissues. However, several brain tumor samples involving oligodendrocytes as well as some GBM samples showed a similar level of reflectance in the red (*i.e.* 600–800 nm) as compared to that of white matter *in vivo*, which contradicts this expectation. Edema in white matter and calcification and/or necrosis in brain tumors are suspected to be responsible for this deviation. Measurement of the optical properties of brain tissues *in vivo* is currently in progress to identify the cause(s) of high scattering in certain tumor samples.

Although it was confirmed *in vitro* as well as *in vivo* that fluorescence alone was insufficient for brain-tissue discrimination, empirical algorithms based on combined fluorescence and diffuse-reflectance spectroscopy were able to differentiate normal brain tissues from tumor/tumor margin tissues with high sensitivity. F/Rd_{460} and Rd_{625} were the *in vivo* discrimination criteria used in this preliminary analysis. F/Rd_{460} separates gray matter and tumor tissues, while Rd_{625} separates white matter and tumor tissues. The advantage of using F/Rd_{460} as compared with F_{460} is that it reduces the effect of blood contamination (17–20). However, this approach is successful only when the degree of blood contamination is moderate. Therefore, it is extremely important that spectral measurements are repeated after recleaning the investigated site and probe, when pronounced blood-absorption signatures are observed in the diffuse-reflectance spectrum.

A more effective discrimination (*i.e.* yielding a higher sensitivity) could be achieved by using F/Rd_{460} and Rd_{625} in a two-step algorithm. This was achieved by first separating all the investigated samples according to their Rd_{625} and then treating each subgroup with a second separate discrimination criterion (see Figs. 3 and 4). This approach was especially effective in differentiating ITM from normal brain tissues. This enhancement is attributed to the fact that using Rd_{625} initially separates the samples with high reflectance thus improving classification along the Rd_{625} axis. For the same reason this discrimination method also yielded an improved sensitivity in separating normal brain tissues from primary tumors. However, the differentiation of secondary tumors was not enhanced, as both misclassified secondary tumor samples were along the F/Rd_{460} axis (see Fig. 3c).

One possible cause for tissue misclassification may be due to an error in the site of biopsy as compared to the investigation site. This problem is particularly significant in this case as the investigation volume, determined by the sensing area of the optical probe (*i.e.* approximately $600 \times 670 \mu\text{m}^2$) and the penetration depth of the excitation light (*i.e.* less than $500 \mu\text{m}$), is very small. In addition to biopsy error, different degrees of blood absorption in the fluorescence signal as compared with the corresponding diffuse-reflectance signal of the same site as a result of progressive blood contamination may also cause tissue misclassification. However, the most significant cause may be due to the limited information that is used in the algorithms developed here. The empirical

discrimination algorithms have two important limitations. First, clinically useful diagnostic information is typically contained in more than just the few wavelengths surrounding the peaks or valleys of optical spectra observed in tissue; a method of analysis and classification that includes all the available spectral information from fluorescence and diffuse reflectance can potentially improve the accuracy of detection. Second, empirical algorithms are optimized for the spectra within the study. Hence, the estimates of algorithm performances will be biased toward that patient population. An unbiased estimate of the performance of the algorithms is required for an accurate evaluation of the performance of optical spectroscopy for tumor-margin detection. To address these limitations, multivariate statistical techniques will be used to develop and evaluate algorithms that differentiate between normal, tumor margin and tumor tissues based on fluorescence and diffuse-reflectance spectra. Such a method will, however, require multiple samples within each tissue category, and thus a larger number of patients need to be studied before it can be implemented.

Thus, a new clinical study is currently in progress at VUMC in order to validate those observations presented in this paper in a larger patient population as well as to increase the number of samples within each tissue category. The results from this study have been used to implement many improvements into the new clinical study. For example, each site is thoroughly flushed with saline to minimize the effect of blood absorption; the surgeon uses sterile gauze to blot the excess fluid and secure the investigated site, which minimizes progressive blood contamination. In addition, the spectral acquisition time has also been shortened. Results from this new clinical study will be published in the future.

Acknowledgments—The authors wish to thank Dr. Peter E. Konrad and Dr. Robert J. Weil for their support and help. The authors acknowledge the financial support of the Laser Fellowship Program from the W. M. Keck Foundation FEL Center, Vanderbilt University, and the Whitaker Special Opportunity Award.

REFERENCES

- Chamberlain, M. and P. Kormanik (1998) Practical guidelines for the treatment of malignant gliomas. *West J. Med.* **168**, 114–120.
- Shapiro, W. and J. Shapiro (1998) Biology and treatment of malignant glioma. *Oncology (Huntingt.)* **12**, 233–240.
- Toms, S. A., D. Ferson and R. Sawaya (1999) Basic surgical techniques in the resection of malignant gliomas. *J. Neurooncol.* **42**, 215–226.
- Wisoff, J., J. Boyett, M. Berger, C. Brant, H. Li, A. Yates, P. McGuire-Cullen, P. Turski, L. Sutton, J. Allen, R. Packer and J. Finlay (1998) Current neurosurgical management and the impact of the extent of resection in the treatment of malignant gliomas of childhood: a report of the Children's Cancer Group trial no. CCG-945. *J. Neurosurg.* **89**, 52–59.
- Hess, K. (1999) Extent of resection as a prognostic variable in the treatment of gliomas. *J. Neurooncol.* **42**, 227–231.
- Barnett, G. H., C. P. Steiner and D. W. Roberts (1998) Surgical navigation system technologies. In *Image-guided Neurosurgery: Clinical Applications of Surgical Navigation* (Edited by G. H. Barnett, D. W. Roberts and R. J. Maciunas), pp. 17–32. Quality Medical Publishing, St. Louis.
- Auer, L. M. and V. v. Velthoven (1990) *Intraoperative Ultrasound Imaging in Neurosurgery: Comparison with CT and MRI*. Springer, Berlin.
- Hill, D., C. J. Maurer, R. Maciunas, J. Barwise, J. Fitzpatrick and M. Wang (1998) Measurement of intraoperative brain surface deformation under a craniotomy. *Neurosurgery* **43**, 514–526.
- Dorward, N., O. Alberti, B. Velani, F. Gerritsen, W. Harkness, N. Kitchen and D. Thomas (1998) Postimaging brain distortion: magnitude, correlates, and impact on neuronavigation. *J. Neurosurg.* **88**, 656–662.
- Richards-Kortum, R. and E. Sevick-Muraca (1996) Quantitative optical spectroscopy for tissue diagnosis. *Annu. Rev. Phys. Chem.* **47**, 555–606.
- Ramanujam, N. (2000) Fluorescence spectroscopy of neoplastic and non-neoplastic tissues. *Neoplasia* **2**, 89–117.
- Bottiroli, G., A. C. Croce, D. Locatelli, R. Nano, E. Giombelli, A. Messina and E. Benericetti (1998) Brain tissue autofluorescence: an aid for intraoperative delineation of tumor resection margins. *Cancer Detect. Prev.* **22**, 330–339.
- Stummer, W., S. Stocker, S. Wagner, H. Stepp, C. Fritsch, C. Goetz, A. E. Goetz, R. Kiefmann and H. J. Reulen (1998) Intraoperative detection of malignant gliomas by 5-aminolevulinic acid-induced porphyrin fluorescence. *Neurosurgery* **42**, 518–525 (discussion: 525–526).
- Lin, W.-C., S. A. Toms, M. Motamedi, E. D. Jansen and A. Mahadevan-Jansen (2000) Brain tumor demarcation using optical spectroscopy; an *in vitro* study. *J. Biomed. Opt.* **5**, 214–220.
- Shim, M. G., B. C. Wilson, E. Marple and M. Wach (1999) Study of fiber-optic probes for *in vivo* medical Raman spectroscopy. *Appl. Spectrosc.* **53**, 619–627.
- Eggert, H. R. and V. Blazek (1993) Optical properties of normal human intracranial tissues in the spectral range of 400 to 2500 nm. *Adv. Exp. Med. Biol.* **333**, 47–55.
- Alfano, R. and N. Zhadin (1998) Correction of the internal absorption effect in fluorescence emission and excitation spectra from absorbing and highly scattering media; theory and experiment. *J. Biomed. Opt.* **3**, 171–186.
- Gardner, C. M., S. Jacques and A. Welch (1996) Fluorescence spectroscopy of tissue: recovery of intrinsic fluorescence from measured fluorescence. *Appl. Opt.* **35**, 1780–1792.
- Wu, J., M. Feld and R. Rava (1993) Analytical model for extracting intrinsic fluorescence in turbid media. *Appl. Opt.* **32**, 3585–3595.
- Zeng, H., C. MacAulay, D. McLean and B. Palcic (1995) Spectroscopic and microscopic characteristics of human skin autofluorescence emission. *Photochem. Photobiol.* **61**, 639–645.